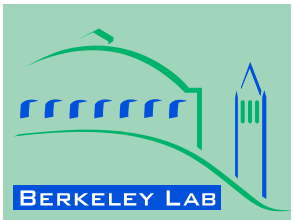


ERNEST ORLANDO LAWRENCE
BERKELEY NATIONAL LABORATORY

# Software-as-a-Service Optimised Scheduling of a Solar-Assisted HVAC System with Thermal Storage

**A. Mammoli[a], M. Stadler[b], N. DeForest[b], H. Barsun[a], R. Burnett[a] and C. Marnay[b]**

**[a] University of New Mexico (UNM)**
**MSC01-1150**
**1 University of New Mexico**
**Albuquerque, NM 87131, USA**

**[b] Lawrence Berkeley National Laboratory (LBNL)**
**1 Cyclotron Road**
**Berkeley, CA 94720, USA**

## Environmental Energy Technologies Division

**presented at the 3rd International Conference on Microgeneration and Related Technologies**
**Naples, 15-17 April 2013**

***http://eetd.lbl.gov/EA/EMP/emp-pubs.html***

This work was supported by the Office of Electricity Delivery and Energy Reliability's Energy Storage and Smart Grid Programs in the U.S. Department of Energy, under contract No. DE-AC02-05CH11231 (LBNL) and through Sandia National Laboratories under PO 570462 (UNM). The authors gratefully acknowledge this support.
.

## Disclaimer

# SOFTWARE-AS-A-SERVICE OPTIMISED SCHEDULING OF A SOLAR-ASSISTED HVAC SYSTEM WITH THERMAL STORAGE

A. Mammoli[a], M. Stadler[b], N. DeForest[b], H. Barsun[a], R. Burnett[a] and C. Marnay[b,*]
[a] University of New Mexico (UNM), MSC01-1150, 1 University of New Mexico, Albuquerque, NM 87131, USA
[b] Lawrence Berkeley National Laboratory (LBNL), 1 Cyclotron Road, Berkeley, CA 94720, USA
*corresponding author: chrismarnay@lbl.gov

## ABSTRACT

The UNM Mechanical Engineering HVAC system incorporates cooling assisted by a 232 $m^2$ solar thermal array providing heat to a 70 $kW_{thermal}$ absorption chiller. A 30 $m^3$ heat storage tank solar decouples heat production and absorption cooling. Additionally, 350 $m^3$ of chilled water storage shifts the cooling electrical load of this high desert location off-peak. While this system already provides substantial energy and cost savings compared to similar conventional buildings, there are still opportunities for improvement. Absorption cooling (augmented by an electrically powered central cooling loop) suffers from parasitic electric loads from a cooling tower pump, a cooling tower fan, and hot and chilled water circulation pumps. Moreover, depending on seasonal, weather, occupancy, and cost conditions, the cold storage tanks may only need partial charging to meet the next day's net building load, and losses need to be considered. Optimally operating this complex thermal-electrical system poses a challenging mathematical problem. A model of the system was built on LBNL's Distributed Resources Customer Adoption Model (DER-CAM) platform. A direct interface between the building energy control system, and DER-CAM hosted on LBNL's server was developed. This interface delivers daily scheduling based on weather forecasts, tariffs, etc., to the building controller. It is found that energy cost savings can be proportionally substantial (almost 30%) - although in this case the payback period for system implementation is long, due to the very low energy consumption of the building. Also, it is found that accurate weather forecasting is a key ingredient of the optimization, although local biases can be corrected for in the optimization.

*Keywords*: absorption cooling, thermal storage, optimisation, software-as-a-service, mixed integer programming.

## INTRODUCTION

Distributed energy resources associated with commercial and institutional buildings are becoming increasingly common, ranging from traditional combined heat and power (CHP) to full-scale microgrids, often capable of supporting the entire facility either in grid-tied or islanded mode. The presence of these distributed systems stems from the need to diversify energy sources to increase reliability, efficiency and sustainability, and to reduce costs. Distributed energy resources can include several forms of generation (including renewables), storage, or load control. Among the possible operating strategies to meet the objectives of providing electric power and thermal conditioning to the facility, the one that optimizes a particular cost function should be chosen. The problem is that determining this schedule involves solving a complex optimization problem with parameters that could change daily as a function of energy prices, weather, occupancy, and other variables. Software-as-a-Service (SaaS) may be an ideal vehicle to perform this task. In this paper, the steps necessary to enable an institutional building to use a remote optimization service, including characterization of the building systems and load profiles, implementation of a data transfer protocol, and modifications to control program, are described. Optimized operation is compared directly with normal un-optimized operation, for various seasonal conditions to determine the cost savings. The sensitivity of the results to accurate weather predictions is assessed.

## METHOD

### Thermal systems characterization

The Mechanical Engineering building at the University of New Mexico (UNM-ME) is a 7000 $m^2$ building energy systems 'living laboratory', located in Albuquerque, New Mexico (USA). The building was commissioned in 1980, but its thermal solar and storage systems received a thorough modernization between 2006 and 2010 [1,2]. During the cooling season (from mid-March to mid-October), the building can be cooled by the thermal cold storage, by a solar-powered absorption chiller, by a district chilled water system, or by various combinations of the above, as shown schematically in Fig. 1.

A four-stage centrifugal pump (P1 in Fig. 1) driven by a variable speed motor circulates a glycol-water mixture through the solar array. A second pump (P2 in Fig. 1), also driven by a variable speed motor, draws water from the bottom of the hot storage tank, routes it through the heat exchanger, and returns it to the top of the hot storage tank. The solar field produces 170 $kW_{th}$ at peak, with an extended peak period resulting from a set of booster mirrors [3], well in excess of the 100 $kW_{th}$ used to drive the absorption chiller's regenerator.

The hot water storage consists of a 30 $m^3$ highly-insulated below-ground unpressurized concrete tank. To measure the parasitic rate of energy loss from the tank, an experiment was performed as follows: The hot tank was charged using the solar heating system, without water draws. The temperature at various tank depths was measured using a tree of calibrated T-type thermocouples.

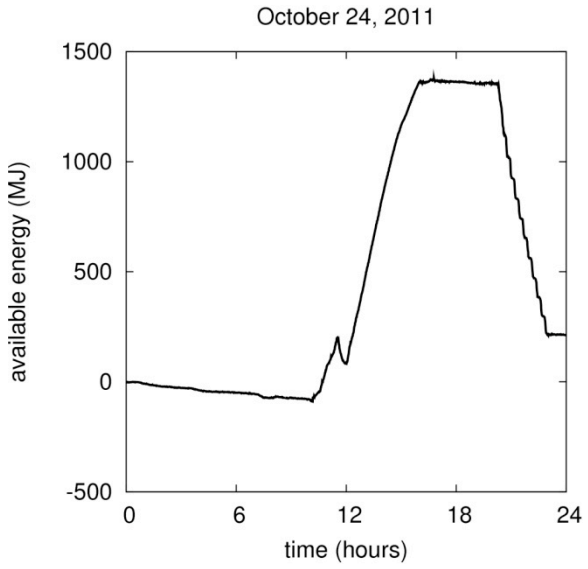


*Figure 2. Energy content of the hot water tank, as a function of time. Note the step-wise change in energy content during the water draw, an artefact from the thermocline going past each thermocouple in the thermocouple tree.*

The tank's total energy content $E_{HS}$ can be accurately approximated using:

$$E_{HS} = \sum_{i=1}^{N} (T_i - T_0) V_i, \quad (1)$$

where $N$ is the number of thermocouples, $T_0$ is an arbitrary datum temperature (here roughly equal to the average temperature of the discharged tank), and $V_i$ is the volume associated with measurement point $i$. The tank energy content is plotted as a function of time in Fig. 2, showing tank charge between 10:00 and 17:00, idle conditions between 17:00 and 20:00, and discharge between 20:00 and 23:00.

While the tank is charged during sunlight hours by the solar array, discharge can occur either during the day or during the nightly off-peak period. An exponentially decaying curve fit to the temperature history during the idle period from 17:00 to 20:00 yields a decay coefficient of 0.3% per hour, indicating a well-insulated tank.

The cooling system can utilize up to seven 50 $m^3$ chilled water storage tanks. Each of which can store approximately 2100 MJ of cooling capacity. To characterize the loss of cooling capacity in the chilled water tanks during the period after charging and before water draw for cooling, one of the seven tanks was instrumented with a thermocouple tree, containing 16 T-type calibrated thermocouples spaced 0.234 m apart.

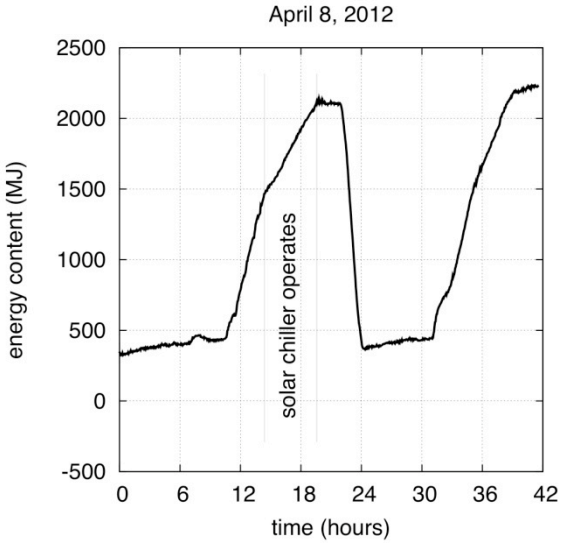


*Figure 3: Energy content of a single cold storage tank operating in isolation, for 42 hours of operation beginning at 0:00 on April 8, 2012.*

The tank loss coefficient was calculated as before, by fitting an exponential decay to the tank energy content history for a period of time when the cold storage is idle, in this case between 0:00 and 7:00. The cold storage degradation rate obtained thus is 0.67% / hour.

The absorption chiller's most energy-intensive process, the regeneration of the Lithium Bromide solution, obtains heat from the hot storage tank at a rate of 100 $kW_{th}$, but there are a number of parasitic energy sinks that result from the need to maintain flows of the Lithium Bromide solution, the heat medium, the cooling water and the chilled water. The 400 W solution pump is internal to the chiller. The heat medium circulation pump (P3) uses 0.8 kW. The cooling water pump (P4) sends water to a cooling tower located on the building rooftop, 21 m above the cooling water level in the sump, using 3.3 kW. The chilled water pump (P5), that draws water from the air handler return and routes it through

the chiller, draws a constant 0.5 kW. The cooling tower fan is rated at 5 kW, but it too is driven by variable speed control, and seldom operates above 50% capacity, corresponding to approximately 0.6 kW.

**Historical building loads**

In this study, only the outside air temperature and the time of day were used to estimate building load. The outside air temperature can be obtained from a weather forecasting service, for example the one posted online by the National Weather Service National Weaher Forecast Office [4]. The building is cooled by chilled water from any combination of three sources: the cold storage tanks, the absorption chiller, and the district chilled water loop. The output of each system is calculated based on relevant historical data collected by the control system for the one-year period beginning on August 1, 2010.

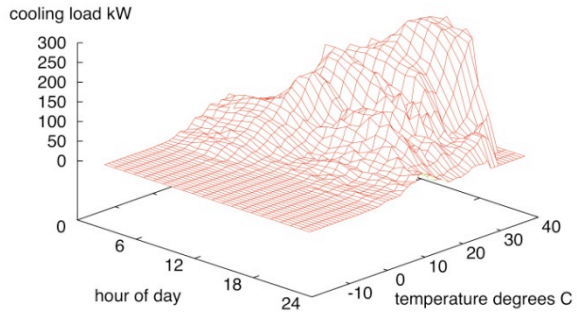


*Figure 4: average building cooling load (thermal) as a function of temperature and time of day, obtained by averaging data over the period August 1, 2010 to July 31, 2012.*

The cooling load is shown in fig. 4 as a function of time of day and ambient air temperature. The shape of the surface follows expectations. There is no cooling load at low ambient temperatures, and the load drops sharply during unoccupied hours, from 19:30 to 7:00. Occasional cooling occurs during unoccupied hours if temperatures in the building exceed a set value. The optimization algorithm calculates a line of best fit or each hour, which is used in conjunction with the predicted ambient air temperature to predict the building load.

## IMPLEMENTATION OF DER-CAM

The HVAC systems at UNM-ME are controlled by two Delta DSC-1616 units. These are fully programmable, native BACnet building controllers that communicate on Twisted-Pair Ethernet 10-BaseT using BACnet IP and BACnet over Ethernet, or on an RS-485 LAN using the BACnet MS/TP protocol. The Delta ORCAView 3.40 system, the interface for the Direct Digital Control (DDC) system at UNM-ME, hosted on a server running the Windows 2008 Server operating system, utilizes the General Control Language Plus (GCL+) language [5], which allows a high level of flexibility in system control and scheduling.

The ORCAView interface has a several roles. First, it serves as a programming platform. Second, it allows a user to monitor system operation in real-time either in graphical or text-based form. Third, it operates a historian that writes system state, at regular intervals and for any desired system variable, to a database (MySQL). Finally, here ORCAView enables communication with DER-CAM.

Every day, DER-CAM obtains information about facilities it serves, including system status, energy tariffs, and weather forecast. In the present case, the sub-system parameters which must be optimized are the absorption chiller schedule, and the cold storage charge level. Because the hot storage tank, which supplies heat to the chiller, and the cold storage tanks, are completely discharged every day, the status of the facility is assumed known. The weather forecast is obtained by DER-CAM directly from the National Weather Service via a XML format once per day. The electricity tariff in New Mexico is fixed Public Service Company of New Mexico electric services [6] for the period of interest. Given this information, DER-CAM produces an optimized set of operating parameters for the week ahead on a daily basis [7], which are embedded in a spreadsheet file, and made available at the LBNL server at 11:00 each day.

The procedure to import the optimization file from the LBNL server to the UNM-ME server, and to transfer the relevant information to the controller, is coordinated by a scheduler, which is part of the 2008 Server operating system, with tasks performed daily as follows:

1. 14:50 - an ftp client is activated. The client obtains the optimization spreadsheet file from the LBNL server. To increase the probability of obtaining the file for the next day's operation, the procedure is repeated two more times, at 14:55 and 15:00.
2. 15:02 - the spreadsheet is moved to a working directory, and archived.
3. 15:04 - Information related to the chiller operating schedule and the cold tank state of charge is copied from the original spreadsheet into a second one which contains only this information.
4. 15:06 - a database program accesses the contents of the spreadsheet file.
5. 15:08 - An Open DataBase Connectivity (ODBC) driver transfers the next night's cold

storage SOC set point and the next day's chiller schedule.

6. 08:00 - the new chiller schedule is copied from a temporary location to the operating location, ready for the day's operation.

The procedure is very flexible, since in principle any amount of needed information could be picked from the DER-CAM spreadsheet file and transferred to the controller using exactly the same process. It should be noted at this point that the framework presented here is in line with the Software-as-a-Service philosophy. The DER-CAM service provides a wealth of information about the system's optimized operation, generally much more than is needed by the end-user. There is a good reason for this - different application may need different information, but rather than customize the output for every single application, DER-CAM produces a standard format which is verbose. The burden of selecting the appropriate information for the system at hand is placed on the end-user, rather than on the optimization host, which could otherwise not cope with the volume of individual applications. On the other hand, selecting the appropriate information subset from the standard DER-CAM output is a small burden for the end-user, who only performs this task once during system setup. This way, by allowing DER-CAM to produce a standardized output, the SaaS costs can be minimized..

## REGULAR VS. OPTIMAL SCHEDULES

The building is heated and cooled via a dual-duct system, with individual air handlers serving their respective zones. The air handlers are scheduled to begin operating at 7:00, and stop operating at 19:30, roughly reflecting the occupancy of the building. When the outside air temperature is greater than the set discharge temperature, the air handlers request cooling water from the system. In this instance, the primary cooling pumps (P5 in Fig. 1) begin drawing water from the bottom of the cooling tanks and deliver the water to the cooling coils. If the return temperature from the cooling coils is over 18.3°C, chilled water from the campus district energy system is circulated through the cooling heat exchanger, to maintain the coil return temperature at 65°C.

This circumstance generally arises when the chilled water storage system has been depleted, either due to insufficient charging the night before, or exceptionally hot weather. In addition, when the solar absorption chiller is active, water at 15-18°C is drawn from the cooling coil return, routed through the absorption chiller, mixed with an appropriate amount of water drawn from storage, cooled to 8°C, and re-inserted into the main flow upstream of the cooling coils, thus reducing the load on the chilled water storage.

When operating in standalone mode (i.e. without optimization), the cooling system operation is as follows:

- The cold storage is charged nightly. Water drawn from the top of the cold tanks is routed to the heat exchanger, cooled to a desired temperature, and returned to the bottom of the cold tanks. Charging stops when the temperature of the water from the top of the tanks goes below a set value, indicating full charge.
- The absorption chiller is activated when there is a sufficient amount of water in the hot storage tank to allow 'ride through' of intermittent cloud cover. The chiller stops when the temperature of the hot storage drops below 75°C, i.e. when the hot storage is depleted.

While standalone operation is simple and reliable, it suffers from a number of potential drawbacks. Charging the cold storage tanks beyond what is needed inevitably results in inefficiency, since the tanks are constantly losing some cooling capacity. Similarly, operation of the chiller during the day (i.e. on-peak) may not be optimal. The electrical loads of the hot water circulation pumps, the chiller solution pump, the cooling tower pump, and the cooling tower fan occur at high cost times. Operating the cooling tower during the hottest parts of the day results in higher fan speed. The substantial redundancy in the ability to provide chilled water to the cooling coils allows flexibility in scheduling, without compromising the comfort of building occupants. In the present work, two aspects of system scheduling were considered:

- The cold storage system can be charged only as needed to meet the building load, rather than to full capacity.
- The absorption chiller can be operated partly during the off-peak period, although not entirely since the capacity of the hot storage is not sufficient.

## DAY-AHEAD FORECAST ACCURACY

A typical DER-CAM optimized schedule for one week is shown in Fig. 5. The optimization of the ME building systems schedule is based on temperature and solar irradiance forecasts. The building load is strongly correlated to outside air temperature and time of day.

Inspection of Fig. 4 reveals a cooling load rate of change of 7.7 $kW_{th}$ per °C at noon. An error in

temperature forecast of 1 °C over the course of 5 hours would correspond to an error in building load forecast of approximately 38 $kWh_{th}$.
The solar irradiance forecast, on the other hand, serves to predict the total length of time that the absorption chiller will be active during the following day. Optimization usually favours operation of the chiller during off-peak times, but because the hot storage is not large enough to store the entire daily heat production of the solar array, some on-peak operation is necessary.
The relation between forecast and actual weather parameters is shown in Fig. 6. The temperature forecasts tend to under-predict lower temperatures, and over-predict higher temperatures, as indicated by the negative y-intercept and the larger than unity slope of the linear fit.

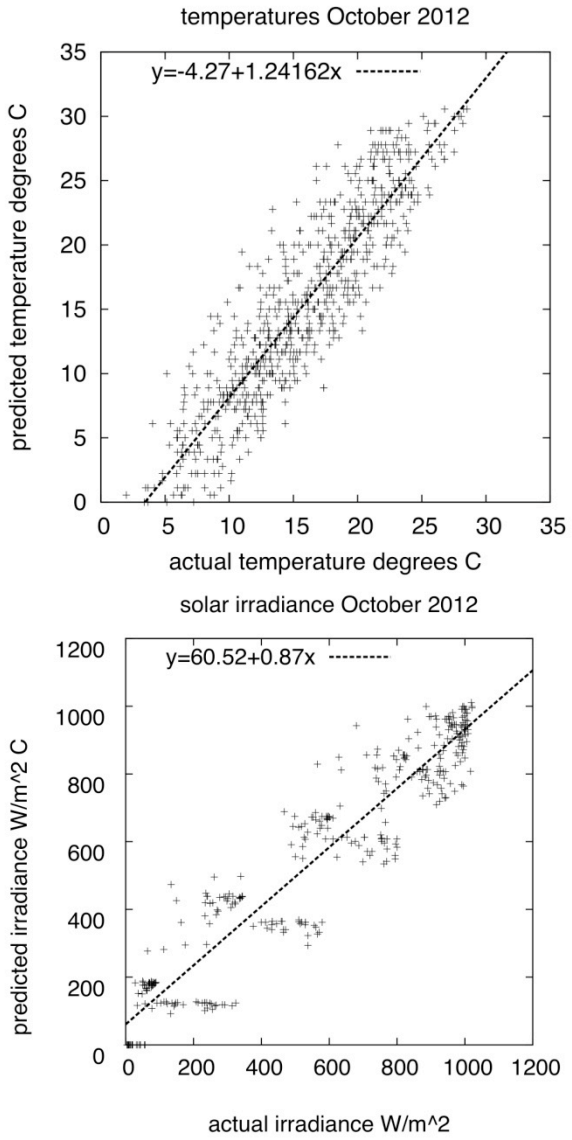


Figure 6: global fits of actual vs. day-ahead forecast temperature (top) and solar irradiance (bottom).

The irradiance forecast is obtained using the NWS cloud cover prediction. A model of the form:

$$I_p = I_c(a - bC), \quad (2)$$

where $I_p$ is the predicted irradiance, $I_c$ is the clear-sky irradiance for the date and time, $C$ is the cloud cover prediction (with 0 representing clear sky, and 1 representing completely overcast conditions). The parameters $a$ and $b$ were obtained by minimizing the squared error between actual daily solar energy and the model prediction. For the present case, they are 1.0 and 0.39. The scatter plot of actual vs. predicted irradiance in Fig. 6 shows an over-prediction of low irradiance and a slight under-prediction of high irradiance. The staggered clusters of prediction are likely due to the three-hour long cloud cover forecast blocks.
Redundancy must be allowed to account for possible inaccuracy in the forecast. For the case of the cold storage, under-prediction of the building load would simply result in additional cooling drawn from the district energy system when the cold storage is depleted. Over-prediction of the load, on the other hand, would mean that some of the cold storage capacity would be dissipated by tank losses before further use during the subsequent charge cycle.
For the case of the chiller, under-prediction of the solar energy available would result in overcharging of the hot storage. The control program was modified so that when excessive tank temperatures are detected, the chiller is activated for an hour, irrespective of schedule, returning the hot storage to safe conditions.
An example of operation of the ME building for standalone operations and optimized operations is shown in Fig. 7. In the case of optimized operations, the chiller operates for part of the time off-peak (after hour 44, which corresponds to 20:00). Also, during on-peak operation, the chiller starts and stops three times. Two of the start-stop cycles are due to the safety override due to tank overheating, resulting from under-prediction of the solar irradiance on that day. The following day, during standalone operation, the chiller operates continuously on-peak.

## ECONOMIC ANALYSIS

The application of SaaS described here manages relatively small electric loads and thermal energy storage, so it was known in advance that the cost savings would be limited. The intent of the work was to determine whether, even under these circumstances of limited costs, the implementation of the IT infrastructure necessary to use SaaS for optimization of operations of a medium-size building would be cost-effective.

To estimate costs for implementations where the learning phase is minimal, it is assumed that a modern DDC control system, and the hardware to host the software interface are both already present at the facility. Implementation costs under this scenario result from software (e.g. historian, ODBC interface), programming costs on the client side, and programming costs at the host site. A series of scenarios is presented, representing a broad range of possible applications: a single building, five buildings (e.g. a small commercial retail development), and fifty buildings (e.g. a university campus or a chain of hotels). The costs for the various aspects are summarized in Table 1. The bulk of the cost is in the data collection software and associated interfaces (e.g. the ODBC driver). Also, economies of scale apply in this case: for large enterprises with centralized data collection services (e.g. university campuses, hotel chains, retail chains) these costs are substantially reduced. The second largest cost, associated with tailoring of the optimization software to the particular application at the host site, can also decrease with increasing number of implementations. Here, learning is assumed to follow an 85% experience curve [8].

It is also noteworthy that the implementation cost at the facility is a relatively small component of the total implementation cost, although its share grows as the other costs decrease. Learning for this cost component does apply because, after a small number of prototypes, implementation costs are simply a function of the number of hours needed to implement the interface, which are not likely to decrease since buildings, their mechanical components and thus their control programs, are generally one-offs.

The economic benefits of implementing SaaS operation optimization are strongly influenced by local electricity tariffs. For example, New Mexico's PNM rate 15B [6], specific to large university campuses, applies relatively low energy prices, and a moderate differential between on-peak and off-peak conditions. Typical commercial California energy charges (SCE and SDG&E) are substantially higher, and also include shoulder rates, rather than just on- and off-peak rates. The economic benefits of the present DER-CAM implementation for an individual building are assessed using these three rates, shown in Fig. 9. The optimization performed by DER-CAM for this experiment was based on the PNM rate 15B, and the results may have differed if the other tariffs had been used. However, the differences would have been relatively small, and would have resulted in slightly higher economic benefits.

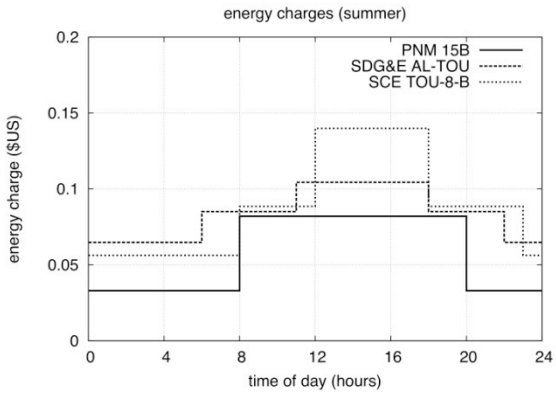


*Figure 9: Energy charges and for Albuquerque, New Mexico (PNM rate 15B) and two service areas in California (rates SDG&E AL-TOU and SCE TOU-8-B) for summer period.*

The first experiment was performed for the two-week period beginning on July 16, 2012, representing summer conditions (June, July and August). For the first week, the building energy systems were operated with no optimization. Specifically, the cold storage was charged fully every night, and the absorption chiller operated on-peak. In the second week, the system was switched to DER-CAM optimization. The cold storage was charged partially, and the operation of the absorption chiller was operated partially off-peak. The operating costs for the two cases are shown in detail in Table 2.

During the shoulder season (the second half of March to May, and September and October), cooling requirements are smaller, and there is even greater opportunity for savings by not fully charging the cooling tanks. Since only a small portion of the tank capacity is needed, fully charged tanks would present an un-necessarily large cold surface area for heat conduction into the cold storage, serving no useful purpose. Costs associated with shoulder-season standalone and optimized operation, for typical weeks, are shown in Table 3. Weekly energy cost savings are shown in Table 4. For the summer season, the cost saving are $43, $81 and $72 for the PNM, SDG&E and SCE tariffs respectively. The shoulder cost savings are $9, $27 and $22 for PNM, SDG&E and SCE respectively. Assuming 18 weeks of shoulder season and 12 weeks of summer season, the yearly savings on cooling are $678, $1,458 and $1,260 for the PNM, SDG&E and SCE tariffs respectively. Irrespective of tariff, the expected yearly percentage energy cost reduction from optimized operation is approximately 29%.

In the worst-case scenario, that of an implementation on a single building with PNM rates, the cost recovery period based on simple payback is 33 years. In the most attractive scenario, with a 50-building implementation and

SDG&E tariff, the payback period drops to approximately 5 years. Does this mean that SaaS is not an attractive proposition for small enterprises? It must be kept in mind that this analysis was performed on a building with very low energy consumption and correspondingly low energy costs, which already placed low bounds on the absolute value of the cost reduction. Regardless, despite the fact that the SaaS model is already very efficient, it appears that further benefits should be sought. For example, embedding the interface developed in the present exercise in the control software directly by the control system vendor would minimize the client-side costs. In addition, it may be possible, if the SaaS model takes hold, to take advantage of utility-side benefits which are only partially embedded in existing tariff structures, particularly if storage systems are part of the optimization [9].

## CONCLUSIONS

The SaaS framework was applied to a medium-sized facility with thermal storage and solar-assisted HVAC for the purpose of optimizing its energy system operating schedule using LBNL's DER-CAM system, to determine cost savings, and compare these with implementation costs.

The optimization involved shifting a few kW of electric loads, and setting the state of charge of the cold storage to meet the expected building load. It was shown that the energy costs to cool the facility during shoulder and summer seasons could be reduced by almost 30%, largely thanks to improvements in the cold storage efficiency. However, because the base- line energy costs for this facility were relatively low, the payback period for a single implementation is not attractive. Multiple similar implementations (e.g. for a hotel chain) would substantially reduce the unit cost, and the payback period would then become attractive.

It was found that the accuracy of the schedule depended strongly on the accuracy of the weather forecast, especially in the case of the amount of solar power available to drive the absorption chiller. Initially, the model often under-predicted the amount of solar heat available, resulting in multiple chiller start/stop cycles during the on-peak period. A later adjustment of the model based on statistical correlation of actual solar heat and predicted solar heat resulted in improved scheduling.

It was not possible to reduce demand charges in this exercise, since the hot storage was not sufficient to shift the entire electrical load due to the operation of the absorption chiller off-peak. However, for the case of multiple facilities behind a single meter, a reduction of the collective peak would be possible using appropriate coordination, without impact on comfort of building occupants. Better economic benefits could arise if utility benefits could be monetized beyond single-meter tariff, for example by aggregating the optimization of multiple facilities.

## ACKNOWLEDGMENTS

This work was supported by the Office of Electricity Delivery and Energy Reliability's Energy Storage and Smart Grid Programs in the U.S. Department of Energy, under contract No. DE-AC02-05CH11231 (LBNL) and through Sandia National Laboratories under PO 570462 (UNM). The authors gratefully acknowledge this support.

## REFERENCES

[1] M. Ortiz, H. Barsun, H. He, P. Vorobieff, and A. Mammoli. Modeling of a solar-assisted HVAC system with thermal storage. Energy and Buildings, 42(4):500–509, 2010.

[2] A. Mammoli, P. Vorobieff, H. Barsun, R. Burnett, and D. Fisher. Energetic, economic and environmental performance of a solar-thermal-assisted hvac system. Energy and Buildings, 42(9):1524–1535, 2010.

[3] C. Armenta, P. Vorobieff, and A. Mammoli. Summer off-peak performance enhancement for rows of fixed solar thermal collectors using flat reflective surfaces. Solar Energy, 2011.

[4] National Weaher Forecast Office. Point forecast: Albuquerque NM. http://forecast.weather.gov, 2012.

[5] Delta Controls. ORCAview Version 3.33 Technical Reference Manual, 2006. Chapter 11 - GENERAL CONTROL LANGUAGE.

[6] Public Service Company of New Mexico electric services. 8th revised rate no. 15B, large service for public universities ≥ 8,000 kW minimum with customer-owned generation facilities served at 115 kV. http://www.pnm.com/regulatory/pdf electricity/schedule 15 b.pdf, August 2012.

[7] C. Marnay, G. Venkataramanan, M. Stadler, A.S. Siddiqui, R. Firestone, and B. Chandran. Optimal technology selection and operation of commercial-building microgrids. IEEE Trans. On Power Systems, 23(3):975–982, 2008.

[8] R.M. Grant. Contemporary Strategy Analysis. Wiley, 2010.

[9] J. Eyer and G. Corey. Energy storage for the electricity grid: Benefits and market potential assessment guide: A study for the DOE energy storage systems program. Technical Report SAND2010-0815, Sandia National Laboratories, 2010.

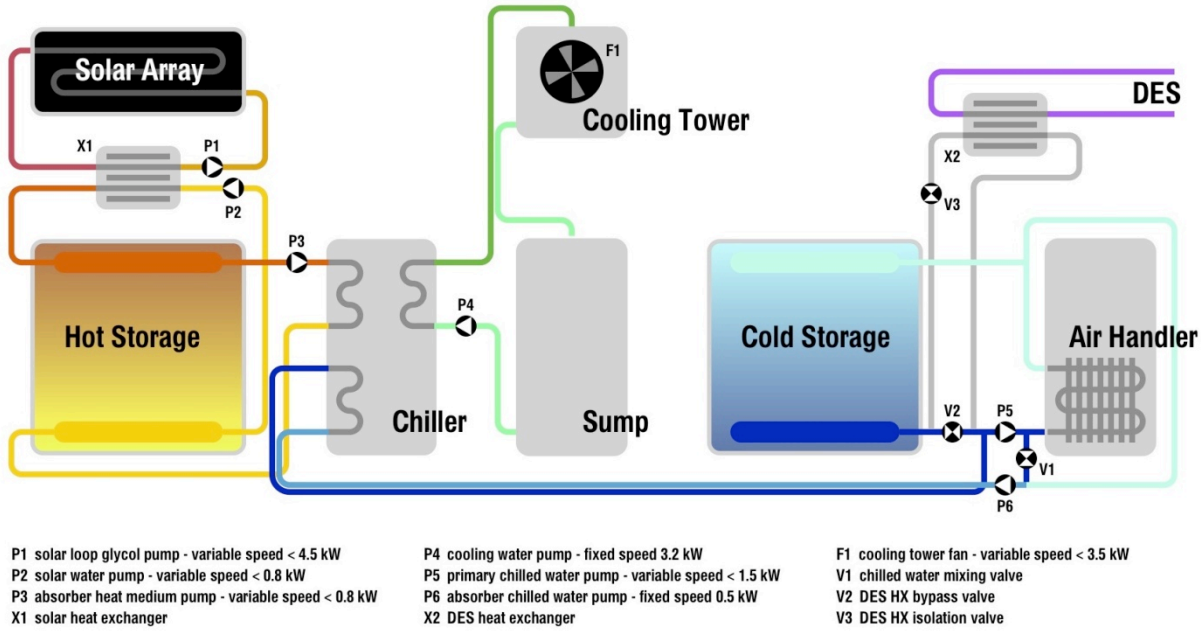


*Figure 1: Schematic representation of the solar-assisted HVAC system at UNM-ME. The hot loop (orange-red) consists of a 30 $m^3$ hot water storage system, a 170 $kW_{th}$ hybrid solar array consisting of 124 $m^2$ of flat plate solar collectors, and 108 $m^2$ of evacuated solar collectors, coupled by a brazed-plate heat exchanger. The array side of the loop is pressurized, while the storage side is not. The cooling loop (green) consists of a 5 $m^3$ sump and a rooftop cooling tower. The chilled water system (blue-purple) consists of 7 tanks, with total capacity of 350 $m^3$. The tanks and an absorption chiller deliver water to air handling units.*

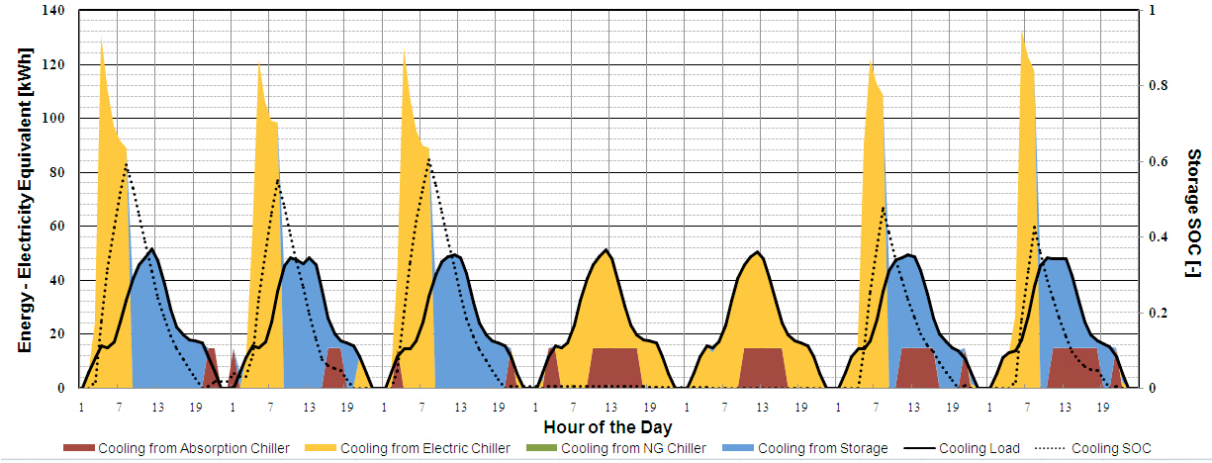


*Figure 5: Typical weekly schedule produced by DER-CAM for UNM-ME.*

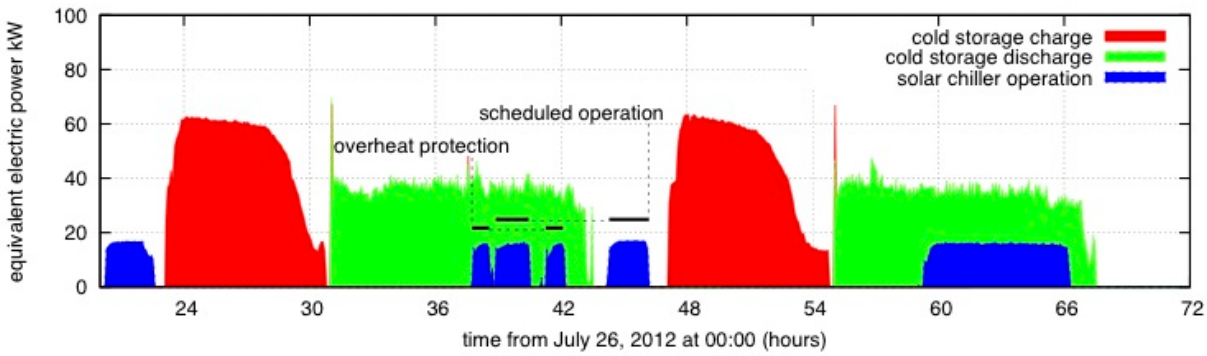


*Figure 7: Comparison of optimized (hours 0 to 48) and standalone (hours 48 to 72) building operations, during peak cooling season in July 2012. Note the difference in operation of the chiller, and the more abrupt cut-off of cold storage charge in the case of optimized operation. Note that, while in general charge time is shorter for optimized operation, in this case the cold storage was not depleted completely during the first day, so charging during the second day was shorter.*

*Table 1: Costs for implementation of the DER-CAM SaaS infrastructure for various typical scenarios.*

| | | | |
|---|---|---|---|
| software costs | Historian + ODBC driver | small<br>medium<br>large | $8,750<br>$15,750<br>$28,500 |
| programming (client side) | | person-hours @ $85.39/hr | item cost |
| | data collection & analysis | 8 | $683 |
| | ftp interface | 1 | $85 |
| | database interface | 3 | $256 |
| | database to DDC | 4 | $342 |
| | control program mods | 8 | $683 |
| | TOTAL | 24 | $2,049 |
| programming (host site) | for first new facility | | $12,000 |
| total unit cost | scenario 1: single building, small software | | $22,799 |
| | scenario 2: 5 buildings, medium software | | $13,427 |
| | scenario 3: 50 buildings, large software | | $7,415 |

*Table 2: Comparison of operating costs in standalone and optimized operation for typical summer weeks. For the SDG&E and SCE rates, the off-peak rate which applies to the chiller is the average of the mid-peak and off-peak rate.*

| | CONTROL<br>begin July 16 2012 for 7 days<br>no DER-CAM | | | | EXPERIMENT<br>begin July 23 2012 for 7 days<br>DER-CAM engaged | | | |
|---|---|---|---|---|---|---|---|---|
| | chiller hours | | DES ton-hours | | chiller hours | | DES ton-hours | |
| | on-peak | off-peak | on-peak | off-peak | on-peak | off-peak | on-peak | off-peak |
| Mon | 5.67 | 0.00 | 0 | 807 | 5.67 | 0.00 | 0 | 522 |
| Tue | 6.83 | 0.00 | 0 | 824 | 3.33 | 2.25 | 0 | 511 |
| Wed | 5.67 | 0.00 | 0 | 606 | 4.00 | 2.00 | 0 | 506 |
| Thu | 7.50 | 0.00 | 0 | 606 | 2.00 | 2.50 | 0 | 506 |
| Fri | 7.00 | 0.00 | 0 | 977 | 4.16 | 2.0 | 0 | 551 |
| Sat | 0.00 | 6.67 | 0 | 660 | 0.00 | 7.25 | 0 | 514 |
| Sun | 0.00 | 2.50 | 0 | 610 | 0.00 | 7.0 | 0 | 87 |
| week sum | 32.67 | 9.17 | 0 | 5090 | 19.16 | 23 | 0 | 3197 |
| kWh per unit | 5.00 | | 0.65 | | 5.00 | | 0.65 | |
| kWh for week | 163 | 46 | 0 | 3308 | 96 | 115 | 0 | 2078 |
| $/kWh PNM | 0.082 | 0.033 | 0.082 | 0.033 | 0.082 | 0.033 | 0.082 | 0.033 |
| $/kWh SDG&E | 0.100 | 0.075 | 0.100 | 0.065 | 0.100 | 0.075 | 0.100 | 0.065 |
| $/kWh SCE | 0.127 | 0.089 | 0.127 | 0.056 | 0.127 | 0.089 | 0.127 | 0.056 |
| $/week PNM | 13.41 | 1.50 | 0.00 | 108.45 | 7.87 | 3.77 | 0.00 | 68.12 |
| $/week SDG&E | 16.35 | 3.44 | 0.00 | 214.39 | 9.59 | 8.62 | 0.00 | 134.66 |
| $/week SCE | 20.75 | 4.06 | 0.00 | 186.27 | 12.17 | 10.18 | 0.00 | 116.99 |

*Table 3: Comparison of operating costs in standalone and optimized operation for typical shoulder weeks. For the SDG&E and SCE rates, the off-peak rate which applies to the chiller is the average of the mid-peak and off-peak rate.*

| | CONTROL<br>begin October 8 2012 for 7 days<br>no DER-CAM | | | | EXPERIMENT<br>begin October 15 2012 for 7 days<br>DER-CAM engaged | | | |
|---|---|---|---|---|---|---|---|---|
| | chiller hours | | DES ton-hours | | chiller hours | | DES ton-hours | |
| | on-peak | off-peak | on-peak | off-peak | on-peak | off-peak | on-peak | off-peak |
| Mon | 3.75 | 0.00 | 0 | 250 | 4.67 | 0.00 | 0 | 162 |
| Tue | 5.33 | 0.00 | 0 | 145 | 4.50 | 2.25 | 0 | 149 |
| Wed | 4.83 | 0.00 | 0 | 289 | 4.00 | 2.00 | 0 | 186 |
| Thu | 2.75 | 0.00 | 0 | 261 | 4.16 | 2.50 | 0 | 220 |
| Fri | 2.5 | 0.00 | 0 | 336 | 2.16 | 2.0 | 0 | 210 |
| Sat | 0.00 | 2.83 | 0 | 129 | 0.00 | 4.42 | 0 | 28 |
| Sun | 0.00 | 4.67 | 0 | 31 | 0.00 | 5.0 | 0 | 40 |
| week sum | 19.16 | 7.50 | 0 | 1440 | 19.16 | 23 | 0 | 995 |
| kWh per unit | 5.00 | | 0.65 | | 5.00 | | 0.65 | |
| kWh for week | 96 | 38 | 0 | 936 | 97 | 51 | 0 | 647 |
| $/kWh PNM | 0.064 | 0.033 | 0.064 | 0.033 | 0.064 | 0.033 | 0.064 | 0.033 |
| $/kWh SDG&E | 0.099 | 0.080 | 0.099 | 0.070 | 0.099 | 0.080 | 0.099 | 0.070 |
| $/kWh SCE | 0.078 | 0.065 | 0.078 | 0.053 | 0.078 | 0.065 | 0.078 | 0.053 |
| $/week PNM | 6.15 | 1.23 | 0.00 | 30.68 | 6.25 | 1.67 | 0.00 | 21.21 |
| $/week SDG&E | 9.48 | 3.00 | 0.00 | 92.67 | 9.65 | 4.06 | 0.00 | 64.05 |
| $/week SCE | 7.47 | 2.44 | 0.00 | 73.02 | 7.60 | 3.30 | 0.00 | 50.47 |

*Table 4: Weekly energy cost comparison for standalone and optimized operation, for various electricity tariffs.*

| | summer | | | shoulder | | |
|---|---|---|---|---|---|---|
| | $/week | | reduction | $/week | | reduction |
| | standalone | DER-CAM | % | standalone | DER-CAM | % |
| PNM | 123 | 80 | 35 | 38 | 29 | 24 |
| SDG&E | 234 | 153 | 35 | 105 | 78 | 26 |
| SCE | 211 | 139 | 34 | 83 | 61 | 26 |